

Herculaneum victims of Vesuvius in AD 79

The eruption's first surge instantly killed some people sheltering from the impact.

The town of Herculaneum, lying at the foot of Mount Vesuvius on a cliff overlooking the sea, was buried by a succession of pyroclastic surges and flows (currents of volcanic ash and hot gases generated by collapse of the eruptive column) during the plinian eruption of AD 79. The skeletons of 80 of 300 people who had taken refuge in 12 boat chambers along the beach have now been unearthed from the first surge deposit. We have investigated how these people were killed by this surge, despite being sheltered from direct impact, after its abrupt collapse (emplacement) at about 500 °C on the beach. The victims' postures indicate that they died instantly, suggesting that the cause of death was thermally induced fulminant shock¹ and not suffocation, which is believed to have killed many of the inhabitants of Pompeii and of Herculaneum itself.

The first surge was generated 12 hours after the eruption started². Unlike the subsequent surges, it billowed through the evacuated town of Herculaneum without damaging it and without leaving any deposit or even disturbing small and fragile heat-resistant objects. The surge advanced as a deflating current with low momentum until it reached the 20-metre cliff drop, when its basal, denser component emplaced abruptly on the beach, halted probably by hydraulic-jump effects, bursting into the waterfront chambers and enveloping the people hiding inside.

We have studied 80 intact skeletons unearthed from chambers 5 (3 skeletons out of 14), 10 (40 skeletons), 11 (5 out of 30) and 12 (32 skeletons). Their life-like stance reflects their posture at the time when the first surge emplaced. These individuals, who did not suffer mechanical impact, do not display any evidence of voluntary self-protective reaction or agony contortions, indicating that the activity of their vital organs must have stopped within a shorter time than the conscious reaction time, a state known as fulminant shock¹. The natural posture of the skeletons has been preserved by virtue of the survival of their anatomical bone connections.

The skeletons, entombed in the ash from the first and covered by the subsequent surges, are lying down or partially leaning up to a few tens of centimetres above the chamber floor, probably because of incipient 'floating'. Their positioning indicates that during emplacement the ash must have expanded slightly and then suddenly deflated, becoming denser and engulfing the bodies, cooling them and fixing them in their positions at the same time.



Figure 1 The feet of a child's skeleton recovered from a waterfront boat chamber after being entombed in the first surge of the AD 79 Vesuvius eruption. The toes show hyperflexion (flexor reflex) of the feet (chamber 12, juvenile): proximal phalanges are dorsiflexed, whereas medial and distal phalanges are plantar-flexed. The feet also show a contracture on the longitudinal axis due to both eversion and inversion, with opposition of the first and the fifth metatarsi and toes (scale rule, 10 cm).

Some of the skeletons have articulated fractures, as seen in incinerated bodies^{3,4}, and the inner skull surfaces, cranial openings and unclosed sutures are blackened from the effects of high temperature on the skull cap under increased intracranial pressure. The victims show transversal clear-cut fractures with blackened edges, and longitudinal fractures in long-bone diaphyses or flat bones, as well as cracked tooth enamel, which are also evident after incineration^{4,5}. The patterns of dental enamel cracks and of bone coloration indicate that the victims were exposed to a temperature of about 500 °C, based on observations of fire victims⁶, ancient burnt bones⁷ and human bone tissue, and on teeth heat-treated in the laboratory^{5,8}. This temperature is compatible with the estimated 480 °C determined palaeomagnetically from a tile collected from outside chamber 12.

The observed flexion of the hands and feet (caused by the thermally induced nociceptive or flexor reflex⁹) (Fig. 1) and occasional spine extension of the skeletons are evidence of instantaneous muscle contraction having occurred before the ash bed compacted. The pugilistic attitude characteristic of limb flexures that result from

tendons and muscles shortening post mortem, typical of fire victims and deaths in pyroclastic flows¹⁰, is only apparent on some of the victims.

The signs of bone carbonization and the preservation of joint connections indicate that most soft body tissues were destroyed by the intense heat and then replaced rapidly by ash. A thermodynamic calculation for a chamber filled by 30 people, on average, indicates that a sudden cooling must have occurred inside the chamber as heat from 8 cubic metres of scorching ash passed into the bodies (corresponding to 4.5 m³ of organic matter) over a contact surface area of about 20 m². The heat of the ash was just sufficient to vaporize most of the organic matter, so the initial violent vaporization caused a sudden drop in ash temperature.

This could explain why the most marked thermal effects are limited to teeth and those parts of the bones least protected by fat and tissue, and would also account for the slower disappearance of some residual soft tissue. The strongest thermal effects are exhibited by bones and teeth from people in the less crowded chamber (5), consistent with our thermodynamic results. The lack of partial thermal remanent magnetization in tiles from inside chamber 12, in contrast with the specimen outside, supports the proposed rapid drop in temperature (over a few tens of minutes¹¹).

Our findings indicate that the emplacement of the first surge caused the instant death of these 80 people as a result of fulminant shock¹. They were killed before they had time to display a defensive reaction (in less than a fraction of a second), their hands and feet underwent thermally induced contraction in about one second (estimated time based on the mean conduction velocity of nociceptive C fibres⁹), the positions of their bodies were fixed by the sudden deflation of the ash bed occurring over the next few seconds; their soft tissues were vaporized and the temperature then fell over a few tens of minutes, inhibiting the progress of the pugilistic stance and the disappearance of residual soft tissue.

Giuseppe Mastrolorenzo*, **Pier P. Petrone†**, **Mario Pagano‡**, **Alberto Incoronato§**, **Peter J. Baxter||**, **Antonio Canzanelle¶**, **Luciano Fattore#**

* *Osservatorio Vesuviano, Via Manzoni 249, 80123 Napoli, Italy*

† *Centro Musei delle Scienze Naturali, Museo di Antropologia*, ‡ *Centro Interdipartimentale di Servizio di Analisi Geomineralogiche, and*

Dipartimento di Biologia Evolutiva e Comparata, Università degli Studi di Napoli Federico II,

Via Mezzocannone 8, 80134 Napoli, Italy
 ‡Soprintendenza Archeologica di Pompei,
 Scavi di Ercolano, 80056 Ercolano, Italy
 §Università degli Studi di Napoli Federico II,
 Dipartimento di Scienze della Terra,
 Largo S. Marcellino 10,
 80138 Napoli, Italy
 e-mail: incorona@umina.it
 ||University of Cambridge Clinical School,
 Addenbrooke's Hospital, Hills Road,
 Cambridge CB2 2QQ, UK

1. Brinkmann, B. et al. *Rechtsmedizin* 83, 1–16 (1979).

2. Carey, S. & Sigurdsson, H. *Geol. Soc. Am. Bull.* 99, 303–314 (1987).
 3. Bohnert, M. et al. *Forensic Sci. Int.* 87, 55–62 (1997).
 4. Bohnert, M., Rost, T. & Pollak, S. *Forensic Sci. Int.* 95, 11–21 (1998).
 5. Yamamoto, K. et al. *Bull. Kanagawa Dent. Coll.* 18, 55–61 (1990).
 6. Holden, J. L., Phakey, P. P. & Clement, J. G. *Forensic Sci. Int.* 74, 17–28 (1995).
 7. Holck, P. thesis, Anatomical Institute, Univ. Oslo (1986).
 8. Shipman, P., Foster, G. & Schoeninger, M. *J. Archaeol. Sci.* 11, 307–325 (1984).
 9. LaMotte, R. H. & Campbell, J. N. *J. Neurophysiol.* 41, 509–528 (1978).
 10. Baxter, P. J. *Bull. Volcanol.* 52, 532–544 (1990).
 11. Butler, R. F. in *Paleomagnetism* 319 (Blackwell, Boston, 1992).

High-speed swimming Enhanced power in yellowfin tuna

Tuna are distinctive among bony fish for their elite swimming ability and their muscle anatomy, having loins of red, aerobic fibres deep within the body where other fish have only white, anaerobic fibres^{1,2}. Here we record the performance of the red muscle of yellowfin tuna *in vitro* and *in vivo* to show how this specialized muscle architecture can double the cruising power of these fish, revealing a functional link between this biomechanical design and high-speed swimming.

Active muscle must develop force and shorten in order to do work. In most fish the relative shortening, or strain, of swimming muscle is the product of body curvature and the distance of the muscle from the backbone³ (that is, strain can be accurately calculated as if the body were a homogeneous, bending beam). If a tuna's body deformed like a bending beam, then the red muscle's internal position (Fig. 1a) would limit strain and therefore the work and power produced, a seeming paradox for fish using high-performance locomotion¹.

We measured muscle strain in yellowfin tuna (*Thunnus albacares*) swimming in a large water tunnel. Sonomicrometry transducers were implanted^{3,4} in superficial and in deep red muscle at the longitudinal mid-point of four animals in order to measure muscle shortening directly. We also used videography and beam theory³ to predict muscle strain by assuming that the fish bends as a homogeneous beam (Fig. 1b).

We found that for superficial red muscle there was close agreement between the measured and predicted strain amplitude and phase (Fig. 1c). However, shortening of deep red muscle measured by sonomicrometry in all fish ($\pm 5.31\%$, s.e. 0.63) was almost double that predicted by beam theory ($\pm 2.78\%$, s.e. 0.43), and it lagged behind body curvature by almost 10% of a complete cycle.

Remarkably, this phase difference produces brief intervals in which superficial muscle is lengthening while the adjacent deep red muscle is shortening, and vice

versa. There is thus a large degree of shear between superficial and deep fibres (the net strain is double that in other fish), and consequently an uncoupling of deep muscle strain from local body bending, which is not observed in other fish³.

Using work-loop techniques^{5,6} to quantify work output from muscle strips, we found that the increased strain results in significantly more work (Fig. 1d). Specifically, the average strain in deep fibres measured by sonomicrometry produces twice the work compared with the average strain predicted by local curvature (24.0 versus 12.7 joules per kg per cycle). Using even larger strains ($\pm 8\%$) does not increase work output significantly, indicating that tuna muscles are designed to work near maximum capacity at the strain they experience in the animal.

Tuna swim by restricting lateral undulations to the most caudal body segments, but maintain their sizeable red-muscle mass in the mid-body region⁷. We believe that this is possible because of the novel physical uncoupling of the action of deep red muscle from local body bending shown here. Deep red muscle at the mid-body in yellowfin tuna shortens in phase with body bending some 20% more to the posterior, supporting the idea that the tuna's complex tendon system and elongate myotomes provide a force-transmission pathway to the tail^{8,9}. We find that deep red fibres undergo strains as large as, or larger than, the strains in superficial fibres, allowing much greater work output during swimming than might be expected from their deep location.

The architecture and physiology of tuna muscle allow it to generate more work than is possible in other fish lacking this specialized anatomy. Although this increased power enables the tuna to achieve higher aerobic speeds, it must also burn more metabolic fuel. At aerobic swimming speeds, tuna do maintain a higher total metabolic rate than salmonids of similar size¹⁰, making it hard to draw conclusions about overall efficiency. But the tuna still enjoys an advantage in being able to maintain higher aerobic speeds than its prey.

Stephen L. Katz*, Douglas A. Syme†, Robert E. Shadwick‡

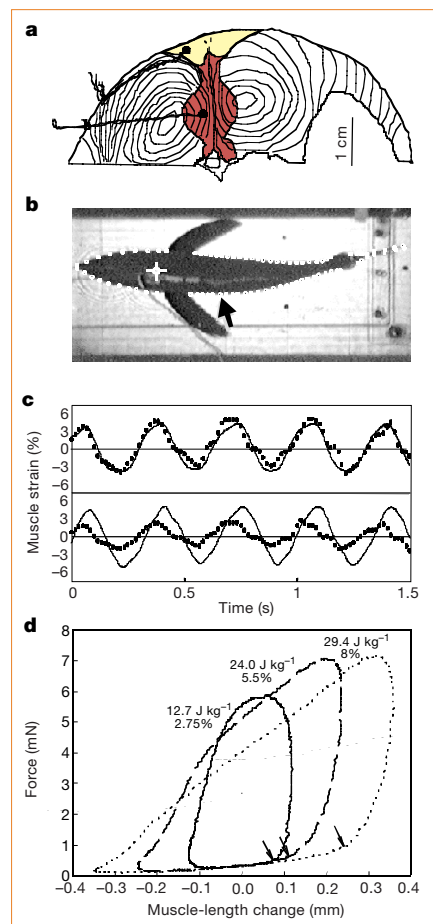


Figure 1 Superior performance of tuna red muscle is due to its anatomical and biomechanical design, as well as to its physiology. **a**, Tuna axial muscle in cross-section; sonomicrometer crystals are shown as black dots with trailing wires. In tuna and non-tuna fish, red muscle forms a wedge close to the skin (yellow), but tuna have red muscle deep in the myotome as well (red). **b**, Video image of a yellowfin tuna swimming at 2.3 body lengths per second. Overlaid digitized points (magnified $\times 5$) were used to calculate body margins and the curvature of the body midline³ and to predict muscle strain from beam theory. Cross, dorsal reflective position marker. Arrow, mid-body position of crystals. **c**, Comparison of red-muscle strain over 4 tailbeats as predicted from videography by beam theory³ (dots) and measured from sonomicrometry (full lines) for tuna swimming at 2.9 body lengths per second (statistics calculated for a minimum of eight tailbeats). Top, peak strain in superficial muscle: predicted, $\pm 4.79\%$; measured, $\pm 4.47\%$ (predicted strain lags behind measured by only 4.69 deg of phase). Bottom, peak strain in deep red muscle: predicted, $\pm 2.41\%$; measured, $\pm 5.46\%$ (measured strain lags behind predicted by 30.7 deg). Orientation of sonomicrometry transducers was verified post mortem. **d**, Work loops from segments of deep red muscle. The muscle was stimulated passively during sinusoidal length oscillations; onset (arrows) and duration of stimulation were adjusted to give maximum net work (loop area), and were similar to activation timing *in vivo*⁹. Loops run anticlockwise, so that the force is relatively low during lengthening and high during shortening. Frequency of the length oscillation (tailbeat frequency) was 3 Hz. Peak amplitude of imposed length change (muscle strain as a percentage of resting length) was $\pm 2.75\%$ (solid line), $\pm 5.5\%$ (broken line), or $\pm 8\%$ (dashed line). The net work done per cycle is shown with the strain for each loop. Muscle resting length, 4.4 mm, corresponding to zero length change on the graph.